

## AtlantECO Deliverable 8.1

### Report on the assessment of future ecosystem drivers, stressors, regime shifts and tipping points

---

Dissemination level: public

Related Work Package	WP8 Predictions of and for Ecosystems services
Related task(s)	Tasks 8.1.1, 8.1.2
Lead beneficiary	CEA & UFBA
Author(s)	O. Jaillon (CEA) & Gillian Ainsworth (USC), Germain Bénard (CEA), Francesco Bosello (CMCC), Donata Canu (OGS), Elisa Delpiazzi (CMCC), Jacobo Feàs (USC), Thomas Froelicher (Unibe), Marion Gehlen (CEA), Ramon Key (CMCC), Simone Libralato (OGS), Katie Longo (MSC), Marco Reale (OGS), Jonathan Rogerson (CEA), Gabriele Standardi (CMCC), Alessandro Tagliabue (ULIV), Marcello Vichi (UCT), Sebastian Villasante (USC), Mathieu Vrac (CEA), Serena Zunino (OGS)
Due date	30.06.2025
Submission date	25.02.2026
Type	Report
Status and version	Final submitted version

**Declaration:** Any work or result described therein is a genuine output of the AtlantECO project. Any other source will be properly referenced where and when relevant.



*This project has received funding from the European Union's Horizon 2020 research and innovation programme under grant agreement No 862923. This output reflects only the author's view and the European Union cannot be held responsible for any use that may be made of the information contained therein.*

## Table of Contents

Executive summary.....	3
1. Introduction.....	4
2. Objectives.....	5
3. Part I – Genomic Insights into Planktonic Vulnerability.....	6
Methodology.....	6
Functional and Transcriptomic Shifts in Eukaryotic Phytoplankton at the Atlantic-Arctic Polar Front (Frémont et al. 2025).....	12
4. Part II – Impacts of Extreme Marine Events on Planktonic Ecosystems.....	17
Introduction.....	17
Study 1 : Increasing Co-occurrence of Ocean Heat and High Acidity Extremes due to Climate Change.....	17
Study 2: Surface and Subsurface Compound Marine Heatwave and Biogeochemical Extremes Under Climate Change.....	19
5. Part III – Evolution of causal relationships under climate change : controls of Net Primary Productivity in the North Atlantic Subpolar Gyre.....	22
Introduction.....	22
Method.....	22
Sliding window approach.....	22
Conceptual scheme.....	23
Results.....	23
Evolving role of stratification.....	23
Nutrient-productivity relationships.....	25
Compensation mechanisms and transport.....	25
Conclusion.....	25
6. General Conclusion and Perspectives.....	27
7. References.....	29



## Executive summary

The Work Package 8 (WP8) of the AtlantECO project focuses on anticipating future changes in basin-scale Atlantic ecosystem services in response to environmental and socio-economic drivers. In alignment with AtlantECO's Objective 4, WP8 aims to deliver a systemic approach to support science-informed decision-making through scenario development, predictive modeling, and integrated analyses of ecosystem health and services. WP8 combines climate projections, biogeochemical models, and socio-economic analysis to evaluate risks of tipping points, regime shifts, and changes in provisioning, supporting, and regulating services such as carbon sequestration, nutrient recycling, and primary production. A significant portion of the results was already achieved prior to the official deadline and presented in previous interim reports and deliverables. However, as this is the final report, these results will be revisited and summarized in the relevant sections to ensure completeness and coherence.

WP8 is structured around four main deliverables, each addressing a critical aspect of the prediction and evaluation of ecosystem services under future climate and socio-economic scenarios. Here we present the deliverable D8.1:

### **Report on the assessment of future ecosystem drivers, stressors, regime shifts and tipping points:**

This deliverable focuses on the identification of future environmental drivers and stressors influencing the Atlantic ecosystems. It integrates analyses of projected climate extremes, the potential for abrupt and irreversible changes (tipping points), and mechanisms driving regime shifts.



## 1. Introduction

The Atlantic Ocean is undergoing rapid and multifaceted changes due to anthropogenic climate forcing. Rising sea surface temperatures, increasing ocean acidification, and declining oxygen levels are reshaping its physical and biogeochemical landscapes, with profound consequences for marine ecosystems and the services they provide. These environmental shifts are neither uniform nor linear—they interact, co-occur, and compound across spatial and temporal scales, challenging the resilience of ocean life and complicating predictions of future ecological states.

In this context and this broader framework, Work Package 8 (WP8) focuses on the foresight dimension: anticipating potential regime shifts, identifying ecosystem tipping points, and assessing the risks posed by multiple stressors to marine biodiversity and function. Deliverable D8.1 contributes to this objective by synthesizing emerging scientific evidence on how Atlantic ecosystems may respond to evolving environmental drivers.

This report integrates three complementary lines of investigation. First, it examines the genomic and transcriptional responses of planktonic communities, the foundational engine of ocean productivity, using high-resolution molecular datasets. Second, it evaluates the occurrence and intensification of extreme environmental events, particularly compound stressors such as concurrent warming and acidification, which pose heightened risks to ecosystem stability. Third, it explores how causal relationships between physical and biological variables may shift under future climate conditions, using a data-driven analysis of primary productivity dynamics in the North Atlantic subpolar gyre.

By combining insights from genomics, climate modeling, and causal inference, this deliverable offers a multidimensional view of future ecosystem vulnerability in the Atlantic. The findings provide not only a scientific foundation for scenario development and risk mapping, but also critical inputs for policy strategies aimed at preserving ocean resilience and functionality in a changing world.



## 2. Objectives

The objective of this deliverable is to assess how Atlantic marine ecosystems may reorganize under future environmental stressors, with a focus on understanding drivers of ecological vulnerability, identifying potential tipping points, and characterizing emerging risks to ecosystem services. This foresight-oriented assessment aligns with AtlantECO's mission to provide science-based guidance for sustainable ocean governance in the face of global change.

To achieve this, the report is structured into three thematic pillars, each addressing a complementary dimension of ecosystem response.

The first pillar focuses on the **biological sensitivity of planktonic communities**, which are fundamental to oceanic food webs and global biogeochemical cycles. Using genomic and metatranscriptomic data, this section aims to evaluate how planktonic provinces are likely to shift spatially under climate change, and how gene expression patterns reflect stress-induced functional vulnerability. It identifies areas where biodiversity and function are most at risk, thereby providing molecular-level early warning signals of ecosystem instability.

The second pillar addresses **compound environmental extremes**, such as the co-occurrence of marine heatwaves, acidification, and oxygen loss. These multivariate stress events are projected to increase in frequency and severity. This section quantifies the extent and intensity of these events under climate change scenarios, and assesses their capacity to undermine biogeochemical stability and precipitate regime shifts in ecosystem structure.

The third pillar investigates how **causal relationships among climate drivers and biological productivity are evolving**. Focusing on the North Atlantic subpolar gyre, this section uses a novel, model-free inference approach to explore how known physical controls of net primary productivity (such as stratification, mixed layer depth, and atmospheric modes like the NAO) may strengthen, weaken, or reverse under climate forcing. The goal is to identify shifts in ecosystem regulation that could signal approaching thresholds or altered states of productivity.

Together, these three dimensions provide an integrated perspective on the vulnerability of Atlantic ecosystems. They allow for a deeper understanding of not just what may change, but how, where, and why changes may unfold—offering critical insight into the resilience and adaptability of marine systems under a rapidly warming climate.



### 3. Part I – Genomic Insights into Planktonic Vulnerability

#### Methodology

This section investigates the vulnerability of planktonic communities in the Atlantic Ocean using two complementary molecular approaches: **genomic biogeography** and **metatranscriptomic functional profiling**. Together, these techniques offer a unique lens through which to assess both the **distributional reorganization** of plankton under climate change and their **functional responses to environmental stressors**.

The first line of analysis, detailed in Frémont et al. (2022), employs metagenomic data from the **Tara Oceans expedition**, spanning 95 ocean stations across the Atlantic and other basins. Genomic provinces were defined based on the genomic composition of eukaryotic and prokaryotic communities using machine learning clustering techniques informed by environmental variables such as temperature, salinity, nutrients, and light availability. These provinces were treated as ecological units and present distinct genomic signatures. The authors then applied ensemble species distribution models (SDMs) to project shifts in these provinces focusing on the year 2100 under RCP8.5 gas emission scenario. Projections were compared against present-day distributions to estimate gain, loss, and spatial displacement of provinces. These spatial patterns were further linked to ecosystem service indicators like primary production and carbon export potential.

The second analytical component, described in Frémont et al. (2025), focuses on the **functional expression profiles** of plankton communities using **metatranscriptomic data** from Tara Oceans samples collected in the Atlantic and in the Arctic Ocean. Gene expression levels were computed. Each sample was associated with environmental measurements to explore correlations between expression patterns and the intensity of physical-chemical stressors, including the effect of marine currents.

By combining spatial projections of **biogeographical turnover** with real-time signatures of **functional stress**, this two genomic approaches allows for an integrated assessment of plankton sensitivity. It provides early-warning indicators of ecological instability by identifying both **where** plankton communities may relocate or collapse, and **how** they functionally respond to compounding stress.

#### Results and Discussion

##### Spatial Reorganization of Plankton Provinces (Frémont et al., 2022)

Frémont et al. 2022 investigates the future restructuring of marine plankton genomic biogeography under anthropogenic climate change, focusing on surface oceans south of 60°N. Using a combination of metagenomic data collected during the Tara Oceans expedition and environmental niche modeling, the authors delineate climato-genomic provinces across six plankton size fractions, from viruses (0–0.2  $\mu\text{m}$ ) to meso-zooplankton (180–2,000  $\mu\text{m}$ ). Each province is defined by specific environmental



conditions and characterized by unique "signature genomes" that correlate with functional and taxonomic distinctions among planktonic communities.

The current distribution of genomic provinces, derived through statistical models applied to World Ocean Atlas climatology data, reveals a marked structuring by size class. Larger plankton size fractions exhibit simpler, zonal biogeographies with clear latitudinal bands, particularly in meso-zooplankton and small metazoans (Fig. 2a–b), while smaller fractions show more complex and patchy distributions, often linked to regional oceanographic features such as gyres and upwelling zones (Fig. 2c–f). A consensus biogeographical map integrating all size classes was generated using the PHATE dimensionality reduction algorithm, providing a comprehensive view of current plankton distribution patterns.

Projections for the end of the 21st century, based on a multi-model ensemble of Earth System Models under the high-emission RCP8.5 scenario, reveal a profound reorganization of these provinces. More than 60% of the ocean area is expected to experience a shift in the dominant province in at least one plankton size class, with smaller size fractions such as protists (0.8–5  $\mu\text{m}$ ) showing the highest turnover rates (up to 31%) (Fig. 3a–d). The most consistent spatial trend is a poleward expansion of tropical provinces and a contraction of temperate ones, driven primarily by sea surface temperature (SST), which accounts for about 50% of the variance in projected changes. Secondary but significant drivers include phosphate and salinity, with local dominance in equatorial and North Atlantic regions, respectively.

The study further investigates functional shifts in key planktonic groups integral to the nitrogen and carbon cycles, focusing on diazotrophs (nitrogen-fixing bacteria), phototrophs, and copepods. Notably, diazotrophic cyanobacteria are projected to increase in abundance across equatorial and tropical zones (Fig 3), suggesting an intensification of nitrogen fixation in oligotrophic regions. This aligns with the projected expansion of specific provinces such as C11, which are enriched in cyanobacteria genomes. While compositional changes in copepods and phototrophs are more spatially heterogeneous, a general trend of increasing subpolar copepods and a redistribution of phototrophic groups is evident.

Crucially, these compositional and spatial changes in plankton communities are associated with measurable shifts in oceanic carbon export. By linking province assemblages to satellite-derived and modeled carbon flux estimates, the authors estimate an average decline of 4% in total carbon export by the end of the century (Fig. 4c). This decrease is especially pronounced in subtropical and equatorial regions and is attributed to losses in nano-diatoms and nano-algae in size fractions 0.8–20  $\mu\text{m}$ . Using the Apriori algorithm, the study identifies significant association rules between community composition changes and carbon flux decline.

Finally, the authors highlight the size-dependent sensitivity of plankton communities to environmental change. Larger plankton appear more responsive to SST alone, while



smaller organisms—more directly reliant on nutrient availability—show stronger sensitivity to changes in phosphate and nitrate concentrations. These findings underscore the differentiated ecological responses across trophic levels and organism sizes, and the necessity of multi-scale genomic and environmental monitoring.

Overall, this work provides one of the first global-scale genomic projections of plankton biogeography under climate change, demonstrating that warming oceans will not only shift species distributions but will also alter fundamental biogeochemical processes such as carbon sequestration and nitrogen cycling. By combining genomics, machine learning, and Earth system modeling, the study offers a framework for future ecosystem projections and highlights the importance of preserving biodiversity and ecosystem function in a rapidly changing ocean.



*This project has received funding from the European Union's Horizon 2020 research and innovation programme under grant agreement No 862923. This output reflects only the author's view and the European Union cannot be held responsible for any use that may be made of the information contained therein.*

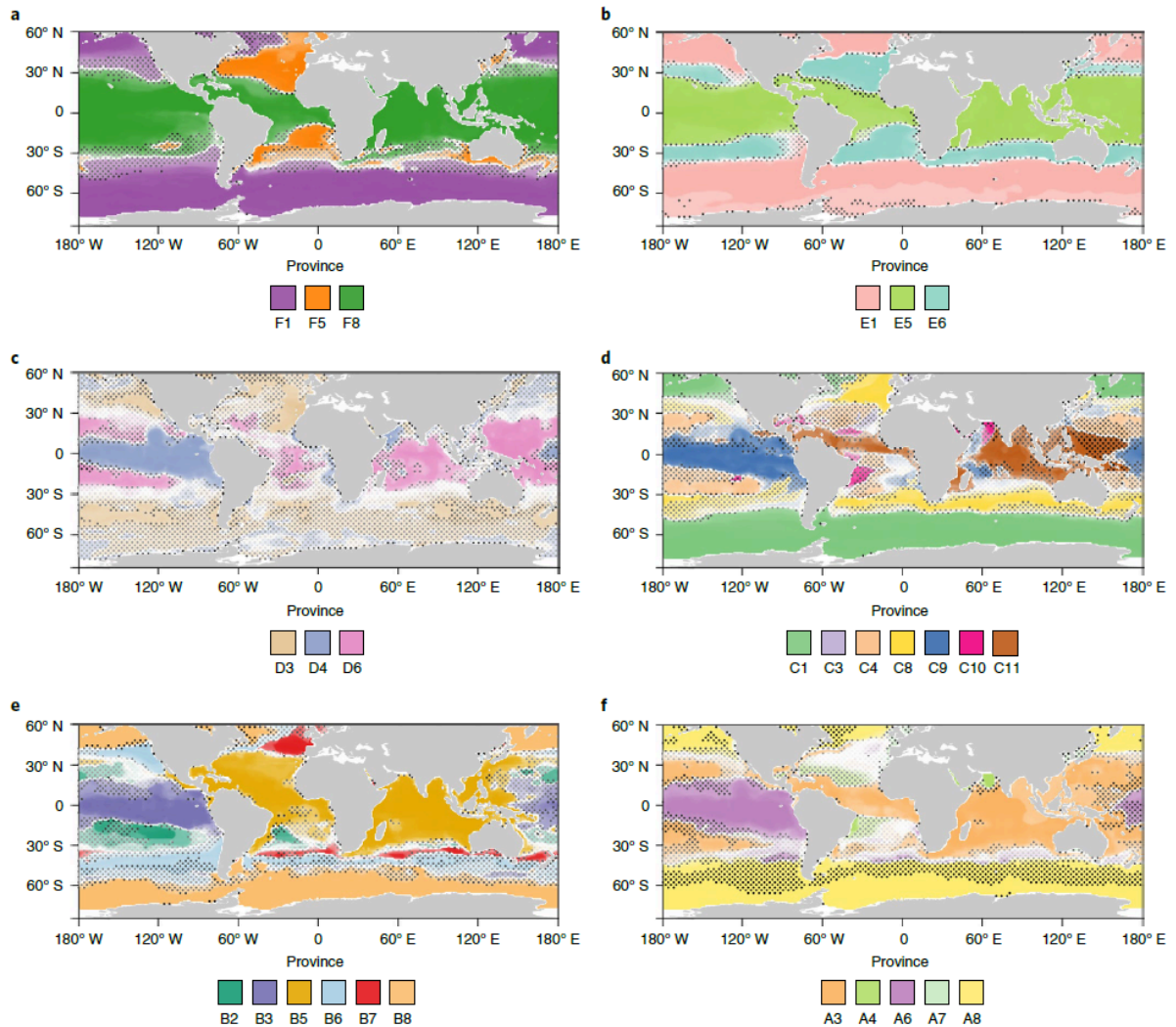


Figure 2 (from Frémont et al. 2022): Global biogeographies of size-structured plankton provinces projected on WOA13 dataset. a–f, Maps showing biogeographies of metazoans enriched (180–2,000  $\mu\text{m}$ ) (a), small metazoans enriched (20–180  $\mu\text{m}$ ) (b), protist enriched (5–20  $\mu\text{m}$ ) (c), protist enriched (0.8–5  $\mu\text{m}$ ) (d), bacteria enriched (0.22–3  $\mu\text{m}$ ) (e) and viruses enriched (0–0.2  $\mu\text{m}$ ) (f) size fraction. At each grid point of the maps, the *dominant* province is represented using a darkness of colour proportional to its presence probability. Dots represent areas of uncertainty (where the delta of probability between the *dominant* and another province is inferior to 0.5). Simple biogeographies are observed in large size fractions ( $>20 \mu\text{m}$ ) with a partitioning in three major oceanic areas: tropico-equatorial, temperate and polar. More complex geographic patterns and patchiness are observed in smaller size fractions.





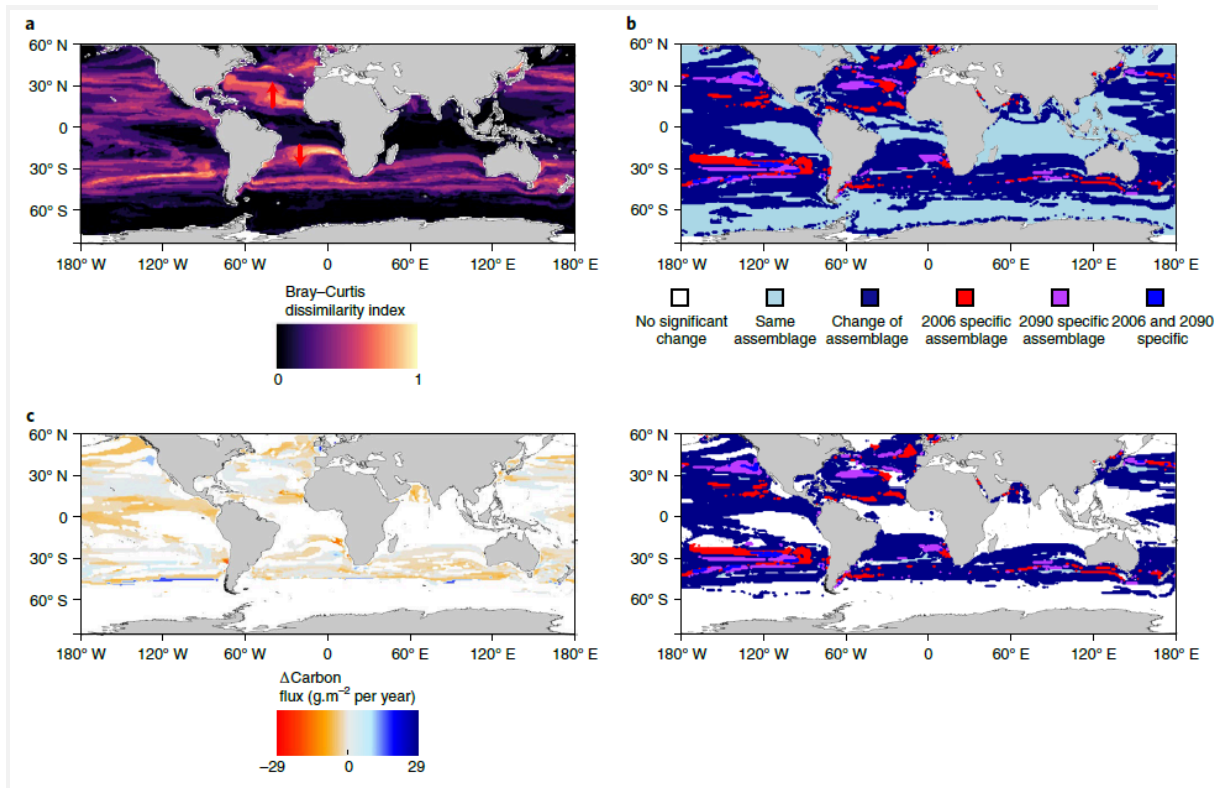


Figure 4 (from Frémont et al. 2022). Fig. 4 | Global impact of climate change on plankton community assemblages and carbon export. **a**, Bray–Curtis dissimilarity index is calculated by integrating all the *dominant* provinces presence probabilities over the six size fractions. **b**, An assemblage is the combined projected presence of the dominant province of each size class. Assemblage reorganization is either mapped on all considered oceans (top) or with a criterion on the Bray–Curtis index (Bray–Curtis > 1/6) (bottom). New assemblages are expected to appear in 2090 (purple + blue), whereas some 2006 specific assemblages are projected to disappear (red + blue). **c**, Difference in carbon export by the end of the century based on present day mean export within each assemblage).



## Functional and Transcriptomic Shifts in Eukaryotic Phytoplankton at the Atlantic-Arctic Polar Front (Frémont et al. 2025)

Frémont et al. (2025) investigated how eukaryotic phytoplankton adapt functionally and transcriptionally as they are transported by ocean currents from the North Atlantic Ocean (NAO) into the Arctic Ocean (AO), with particular focus on the environmental transition occurring at the polar front. This work is based on a comparative analysis of twenty paired metagenomic and metatranscriptomic samples collected across a latitudinal gradient, spanning both basins and intersecting the polar front. The authors tested whether oceanic circulation drives a biological continuum, whether the polar front imposes selective pressures inducing genomic and functional divergence, and whether phylogenetically distinct lineages exhibit convergent transcriptomic responses.

The analysis revealed a strong differentiation in community structure and functional profiles between the NAO and AO, closely aligning with a sea surface temperature transition around 10–15 °C, corresponding to the polar front. This is illustrated in Figure 1A–D, which shows temperature gradients, ocean currents, and associated changes in chlorophyll and net primary production. Genomic diversity, assessed through  $\beta$ -diversity of unigenes (unique genes), showed marked basin-level segregation, while some stations at the front exhibited a mixing of taxa and functions, consistent with physical mingling of water masses. Only about 10% of the ~69 million unigenes were shared between both basins, indicating substantial genomic partitioning (Figure 2A–D).

Functionally, Arctic metatranscriptomes were enriched in processes related to cold acclimation and gene expression regulation. Gene Ontology (GO) terms significantly more abundant in the AO included RNA methylation, tRNA stability, ribosomal biogenesis, and post-translational modification pathways. These processes suggest active cellular strategies to maintain translational fidelity and protein homeostasis under cold conditions. The presence of highly abundant ice-binding domains and other PFAMs related to cold response further supports this.

To disentangle species abundance effects from gene expression regulation, metatranscriptomic data were normalized using corresponding metagenomic profiles. A two-dimensional PHATE embedding of over 570,000 unigenes revealed that gene expression profiles were structured not only by taxonomic lineage but also by basin and environmental parameters such as temperature (Figure 4). Expression patterns were further examined in seven representative metagenomics-based transcriptomes (MGTs) affiliated with major eukaryotic phytoplankton lineages, including Bathycoccus, Micromonas, Phaeocystis, Aureococcus, and a pennate diatom (Minutocellus). These MGTs displayed distinct gene expression levels and responses across basins. For instance, while Bacillariophyta exhibited the highest mean expression, Phaeocystales showed the most consistent photosynthesis-related gene upregulation in the AO, underscoring lineage-specific regulation of primary production.



Crucially, despite taxonomic divergence, multiple phytoplankton lineages exhibited convergent expression responses to temperature decline, especially across genes involved in cold acclimation. Approximately 88,000 unigenes showed expression levels significantly correlated with temperature, with the majority of cold-induced (negatively correlated) responses coming from Bacillariophyta, Mamiellales, and Pelagophyceae. These shared responses included functions such as tocopherol cyclase activity, trehalose biosynthesis, superoxide dismutase, and thiamine diphosphate metabolism, all previously implicated in plant and algal stress adaptation. This convergence indicates the presence of a conserved cold response repertoire among phylogenetically distant eukaryotic phytoplankton.

Overall, this study demonstrates that both community turnover and gene expression plasticity contribute to the restructuring of eukaryotic plankton communities at the Atlantic-Arctic transition. Ocean currents facilitate biological connectivity, yet sharp environmental gradients like the polar front impose selective pressures that drive functional divergence. The results also highlight the capacity of widespread phytoplankton groups to acclimate and potentially adapt to cold environments through shared transcriptional mechanisms. These insights are critical for anticipating changes in planktonic ecosystems under continued “Atlantification” of the Arctic Ocean.



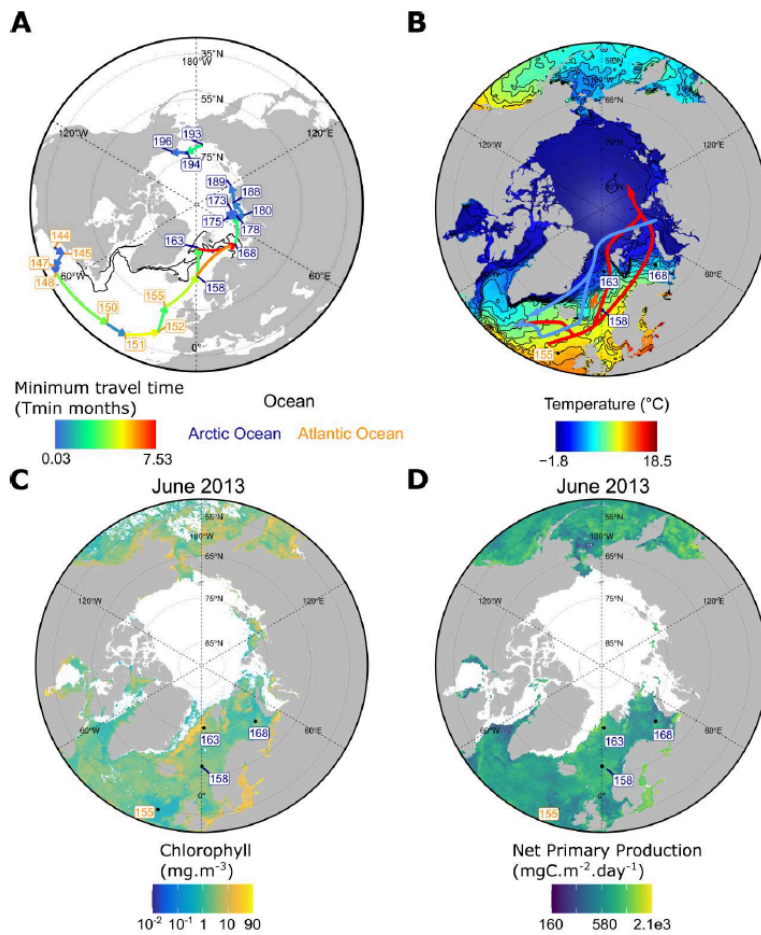
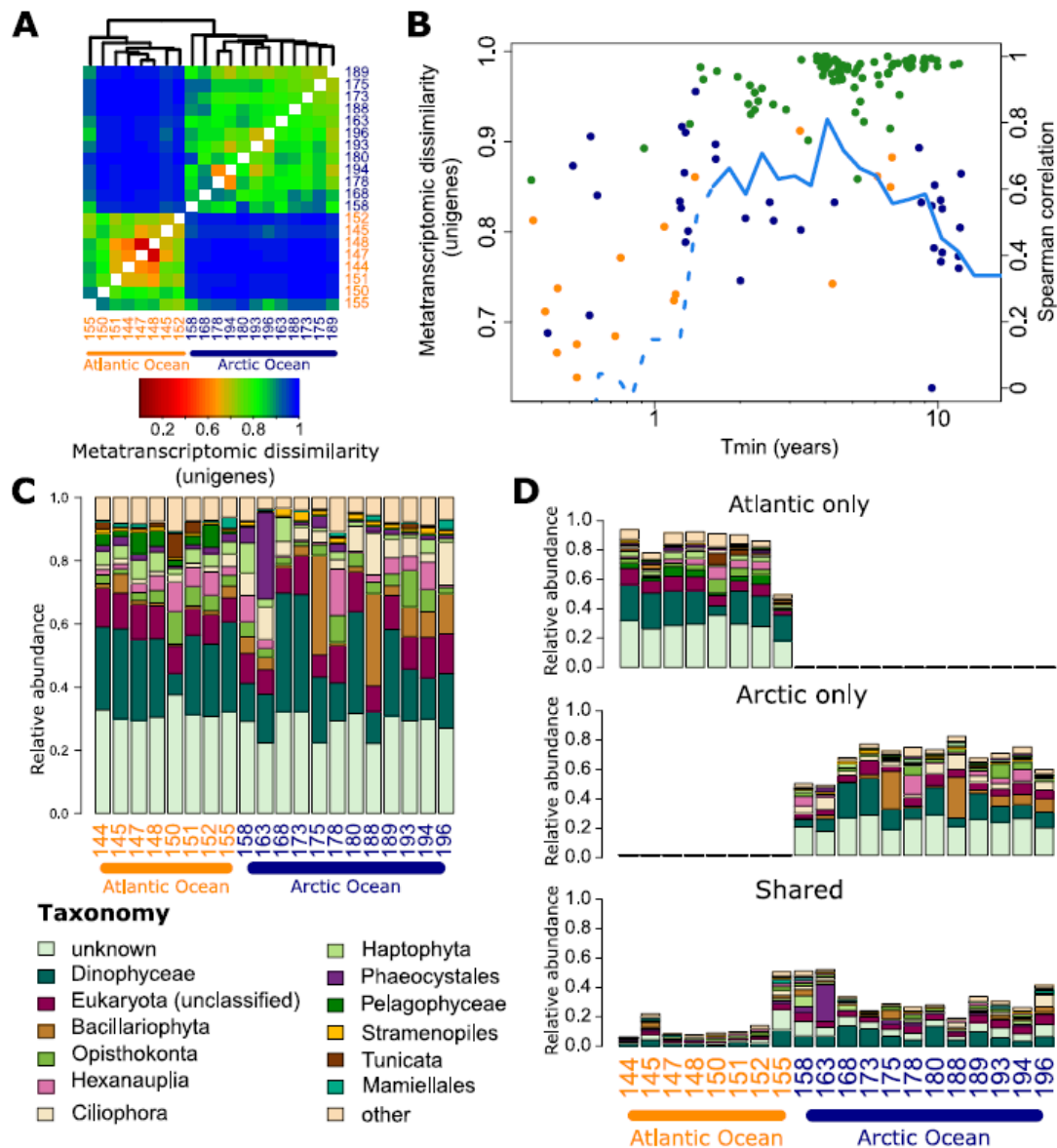


Figure 1 from Frémont et al. 2025. Physical connectivity by currents of studied samples and environmental context of the study. (A) Tara Oceans and Tara Oceans Polar Circle stations considered in this study, and the shortest Lagrangian path (minimum travel time  $T_{min}$ ) between stations, starting at Station 144. (B) Mean Sea Surface Temperature in June 2013 around the time of sampling of stations 155 to 168 (between May and July). The orange arrow indicates the polar front between Stations 158 and 163 where a steep temperature gradient was observed (black lines). Main inflow and outflow currents are represented by red arrows (warm NAO inflows) and blue arrows (cold Arctic outflows). (C) Mean Chlorophyll concentration in June 2013 around Stations 155 to 168. (D) Mean Net Primary Productivity (NPP) in June 2013 around Stations 155 to 168. Chlorophyll and Net primary productivity were computed using an ocean color algorithm developed for the AO. NPP is interpolated from chlorophyll concentrations, resulting in some missing values being filled, while other areas are not interpolated due to masking by sea ice.





**Figure 2** from Frémont et al. 2025. Genomic differentiation of the Arctic Ocean (AO) and North Atlantic Ocean (NAO), its 194 relation to oceanic connectivity and composition of metatranscriptomes. (A) Hierarchical clustering of the matrix of metatranscriptomic pairwise  $\beta$  diversity estimates based on unigene relative abundances (Bray-Curtis dissimilarity index, Methods). (B) Metatranscriptomic diversity as a function of Lagrangian connectivity between pairs of *Tara* Oceans and *Tara* Oceans Polar Circle stations (minimum transport time by currents) and cumulative Spearman correlation coefficient between the two metrics (blue line). When the line is full, the correlation is significant ( $p < 0.05$ ). Orange, dark blue and green points respectively indicate NAO-NAO, AO-AO, and NAO-AO pairs of stations. (C) Metatranscriptomic taxonomic composition based on relative abundances of unigenes from major plankton taxa (taxonomic level can vary) in the NAO and AO (stations ordered by increasing sampling number). (D) Decomposition of the taxonomic composition between basin-specific unigenes and shared unigenes between the two basins (classified based on presence or absence of expression). A clear transition enriched in shared unigenes appears in Stations 155, 158 and 163.



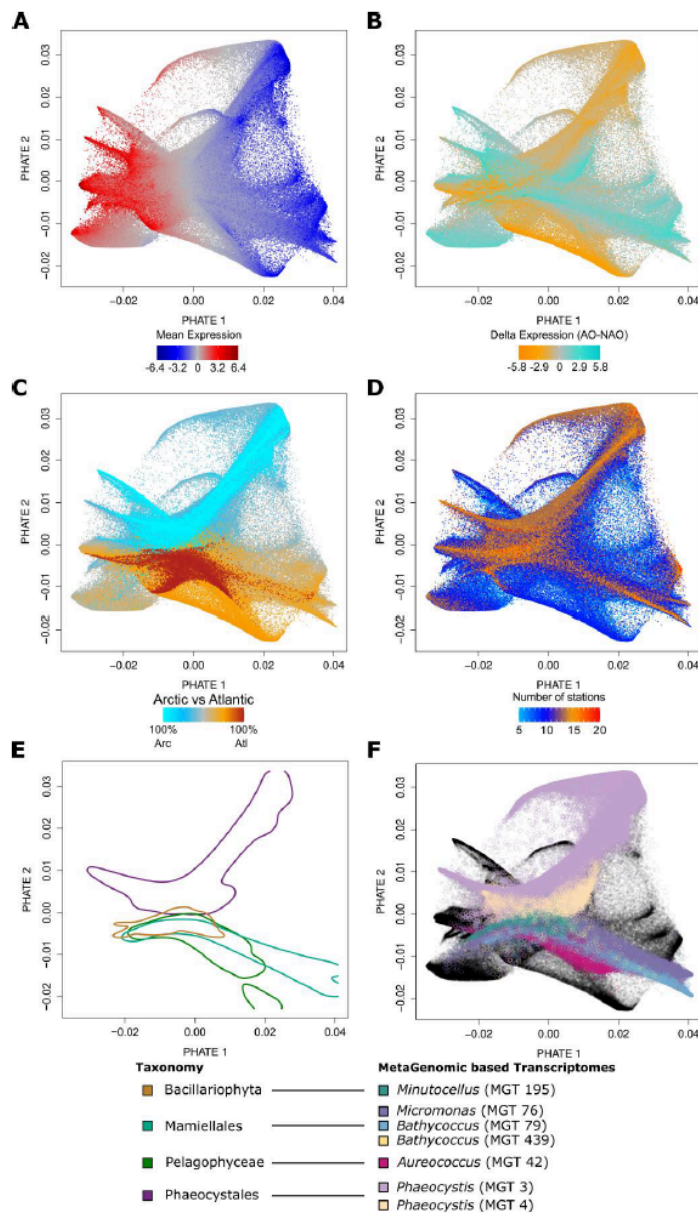


**Figure 4 from Frémont et al. 2025. Topological patterns of the two dimensional embedding of the gene expression matrix.** Each plot shows the same PHATE embedding of the expression matrix of approximately 572,000 unigenes expressed in at least 5 stations. Each point represents the position of the expression profile across the 20 342 samples of one unigene. Each unigene is colored according to different biological and ecological characteristics: (A) Mean level of expression across samples (CLR). (B) Mean delta of expression between the AO and NAO. (C) An index characterizing its biogeography (Methods). (D) The number of stations where unigene expression was detected. (E) Unigene density contours for the main eukaryotic phytoplankton groups analyzed. (F) Seven widespread eukaryotic metagenomics-based transcriptomes (MGTs) are colored in the PHATE space.



This project has received funding from the European Union's Horizon 2020 research and innovation programme under grant agreement No 862923. This output reflects only the author's view and the European Union cannot be held responsible for any use that may be made of the information contained therein.

## 4. Part II – Impacts of Extreme Marine Events on Planktonic Ecosystems

### Introduction

The intensification of climate change is reshaping the frequency, distribution, and severity of extreme events in the ocean, with increasing attention being paid to their compound nature. Unlike isolated anomalies, compound events—such as concurrent marine heatwaves, ocean acidity, and low oxygen event—can exert synergistic and often non-linear impacts on marine ecosystems. These co-occurring stressors compromise the resilience of planktonic communities, disrupt biogeochemical cycles, and threaten biodiversity at multiple trophic levels. While surface impacts have been well-documented, recent studies reveal that subsurface layers are also increasingly affected, highlighting the three-dimensional nature of oceanic stress exposure. The two studies summarized here explore these emerging compound extremes: one investigates the increasing co-occurrence of surface heat and acidity anomalies globally, while the other extends this analysis to include oxygen extremes and their vertical propagation throughout the water column. Together, they provide a multi-layered view of how climate-driven physical and biogeochemical stressors are converging to reshape the ocean's ecological and functional architecture.

### Study 1 : Increasing Co-occurrence of Ocean Heat and High Acidity Extremes due to Climate Change

Burger et al. 2022 investigates the present-day occurrence of compound marine heatwave (MHW) and high acidity (OAX) events using a large ensemble simulation of the GFDL ESM2M model. They also assess how such events are projected to evolve throughout the 21st century. Compound extremes are defined as events in which both SST and hydrogen ion concentration ( $[H^+]$ ) exceed their respective seasonal 90th percentiles. To quantify the increased likelihood of these joint events beyond what would be expected if they occurred independently, the study introduces the "Likelihood Multiplication Factor" (LMF).

Analysis of historical observations and model simulations (Fig. 2) reveal a climatological hotspot of compound MHW-OAX events in subtropical regions. A positive SST- $[H^+]$  correlation is prevalent in tropical and subtropical zones, meaning warmer waters tend to be more acidic due to higher temperature, which outweighs the negative effect on  $[H^+]$  from co-occurring decreases in dissolved inorganic carbon. However, in higher latitudes, this correlation weakens or reverses, reflecting the dominance of decreasing dissolved inorganic carbon. The study also shows that these compound extremes rarely coincide with low aragonite saturation states, an additional key stressor for calcifying organisms, although localized events may still pose significant ecological threats.



Future projections show that by the time the 2 °C global warming above preindustrial levels is reached, the frequency of MHW-OAX days increases by more than tenfold in major ocean basins when using a fixed preindustrial baseline (Fig. 4). Under a shifting-mean baseline, which adjusts for long-term mean changes, the increase is more moderate, but the increase in  $[H^+]$  variability still leads to a small increase in compound MHW-OAX events.

The strong increase of MHW-OAX events under global warming has significant implications: SST anomalies during compound events are in some regions associated with reductions in chlorophyll concentrations, lowered net primary production, and regional shifts in air–sea  $CO_2$  fluxes (Fig. 3a–b). Such changes threaten biodiversity and ecosystem functioning, particularly for organisms like corals, mollusks, and plankton that are sensitive to concurrent thermal and acidification stress.

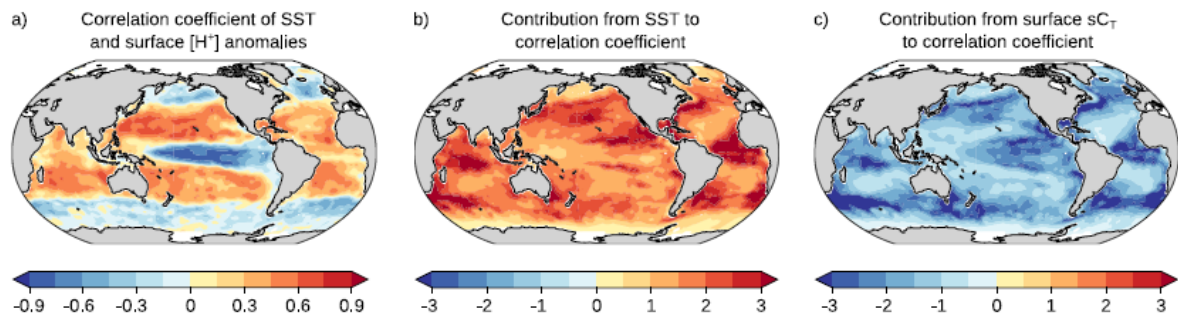
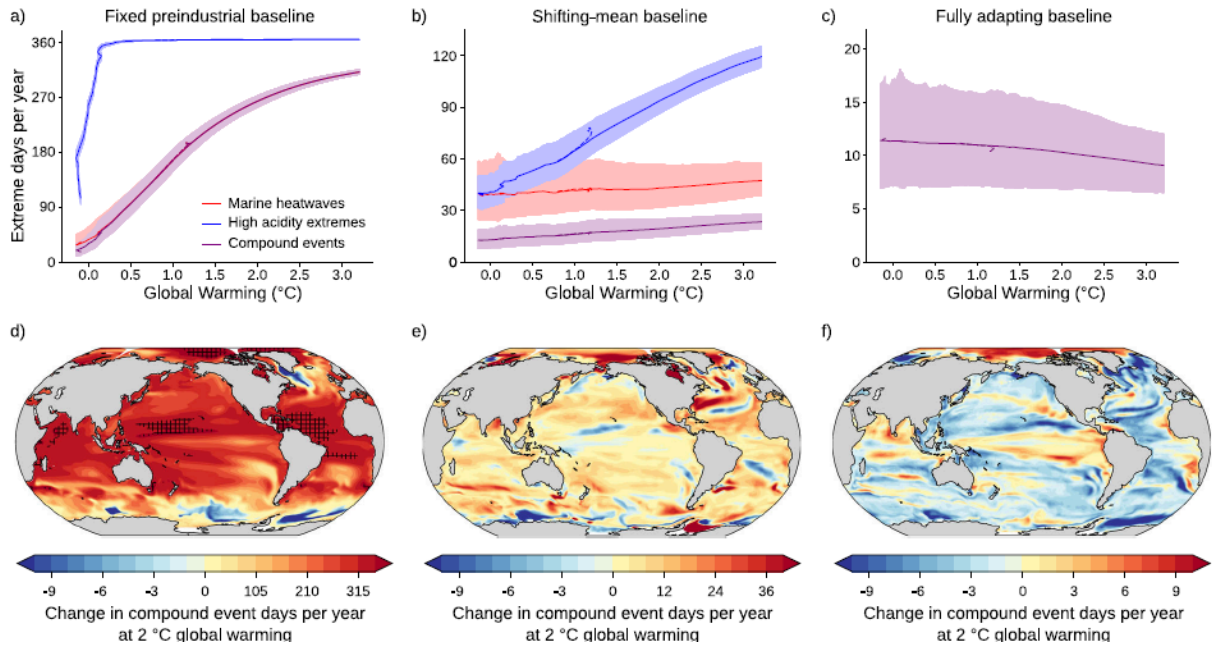


Figure 2 from Burger et al. 2022. The observation-based correlation coefficient of sea surface temperature and  $[H^+]$  anomalies and its drivers from 1982 to 2019. a Pearson correlation coefficient of sea surface temperature (SST) and surface  $[H^+]$  anomalies. The contributions from b variations in SST and c variations in salinity-normalized CT to the correlation coefficient (the sum of panels b and c approximately equals to panel a). The data were linearly detrended prior to the analysis.





**Figure 4** from Burger et al. 2022. Projected changes in the number of MHW-OAX event days per year under global warming. a–c Global-mean number of yearly extreme-event days relative to preindustrial conditions for MHWs (red lines), OAX events (blue lines), and compound MHW-OAX events (purple lines) for a fixed preindustrial baselines, b shifting-mean baselines, and c fully adapting baselines. The time series are smoothed with a 21-year running mean filter. Thick lines display the ensemble means and shaded areas depict the 10th and 90th percentile ranges of the 30 ensemble member simulations over the 1861–2100 period following the RCP8.5 scenario during the period 2006–2100. The dashed lines in a–c show ensemble-mean changes relative to warming levels under the RCP2.6 scenario. Differences between the RCP8.5 and RCP2.6 greenhouse gas scenarios are barely visible because the scenario spread is much smaller than the Ensemble spread, indicating that the projected changes in MHW3, OAX, and compound MHW-OAX events under global warming are independent of the warming path. d–f Regional changes in compound event days relative to the preindustrial period at 2 °C global warming for d fixed preindustrial baselines, e shifting-mean baselines, and f fully adapting baselines. Hatching in d indicates areas with year-round compound events (i.e., more than 360 days per year). Only results of the high-emissions scenario RCP8.5 scenario are shown in d–f, because the changes in globally averaged MHW-OAX occurrence are independent of the warming path.

## Study 2: Surface and Subsurface Compound Marine Heatwave and Biogeochemical Extremes Under Climate Change

Legrix et al. 2025 extend the analysis of compound events to include triple compound events (including low oxygen events - LOX), and expand the focus to the subsurface ocean, reaching depths of up to 2,000 meters. The authors utilize both observational data (2004–2019) and historical and future simulations from the GFDL ESM2M large ensemble.



Spatially, surface MHW-OAX and OAX-LOX events are prevalent in the subtropics (Fig. 2). Vertical patterns are driven by ocean circulation anomalies that displace thermocline waters into deeper or shallow layers, exposing ecosystems eventually to simultaneous thermal, hypoxic, and acidification stress.

Future projections show a sharp rise in the occurrence of single or compound extremes. With 2 °C of warming above preindustrial levels, nearly 98% of the global ocean volume is expected to experience at least one type of extreme or compound event annually under a fixed-baseline approach. Even under a shifting-mean baseline that accounts for gradual adaptation to long-term changes, over 30% of the upper ocean volume will be affected (Fig. 5). Some regions, notably in the Southern Ocean and North Pacific, exhibit local declines in compound event frequency due to regional circulation shifts and biogeochemical buffering.

The study connects these compound extremes with observed ecosystem disruptions. Historical analogs, such as the 2013–2015 Northeast Pacific "Blob" event, illustrate how simultaneous MHW, LOX, and OAX stressors triggered mass mortalities, reduced primary productivity, and disrupted trophic dynamics. The intensification of such events poses escalating risks to fisheries, marine biodiversity, and carbon cycling.

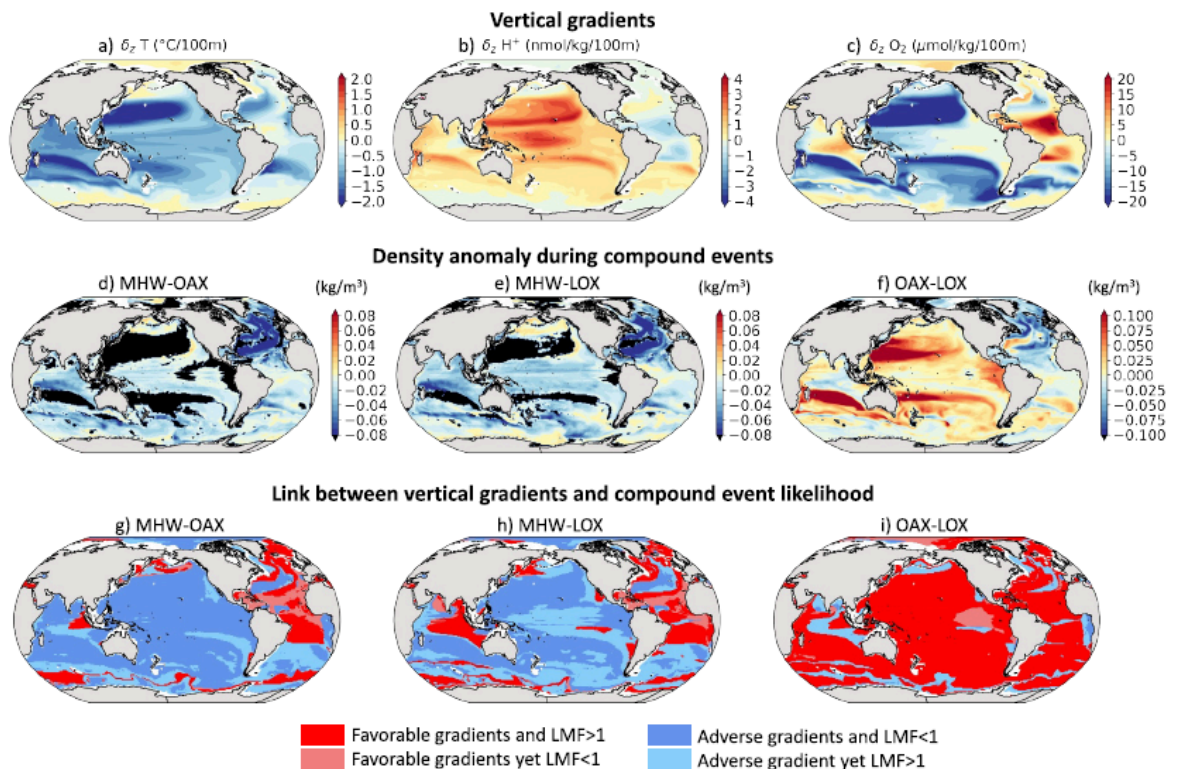


Figure 2 from Legrix et al. 2025. Link between climatological mean vertical gradients of temperature, H<sup>+</sup> concentration, and oxygen concentration, the mean density anomaly during compound events, and



This project has received funding from the European Union's Horizon 2020 research and innovation programme under grant agreement No 862923. This output reflects only the author's view and the European Union cannot be held responsible for any use that may be made of the information contained therein.

compound event likelihood at 617 m in the GFDL-ESM2M-LE. Ensemble mean vertical gradient of (a) temperature ( $\delta zT$ ), (b)  $[H^+]$  ( $\delta z H^+$ ) and (c) oxygen ( $\delta z O_2$ ) concentration over 2004–2019. Ensemble mean anomaly of the potential density referenced to 0 dbar ( $kg \cdot m^{-3}$ ) relative to its seasonal cycle, during (d) compound marine heatwave (MHW) and high acidity (OAX) events, (e) compound marine heatwave (MHW) and low oxygen (LOX) events, and (f) compound OAX-LOX events over 2004–2019. (g) Link between  $\delta zT$  and  $\delta z H^+$  and the likelihood of compound marine heatwave and high acidity (MHW-OAX) events. (h) Link between  $\delta zT$  and  $\delta z O_2$  and the likelihood of compound marine heatwave and low oxygen (MHW-LOX) events. (i) Link between  $\delta z H^+$  and  $\delta z O_2$  and the likelihood of compound high acidity and low oxygen (OAX-LOX) events. Favorable gradients, in red, correspond to regions where (g) T and  $[H^+]$  vary in the same direction, (h) T and  $O_2$  vary in opposite directions, and (i)  $[H^+]$  and  $O_2$  vary in opposite directions, and vice-versa for adverse gradients in blue. Darker colors indicate regions where favorable gradients are associated with frequent compound events (likelihood multiplication factor (LMF)  $>1$ ) and where adverse gradients are associated with rare compound events (LMF  $<1$ ), as expected when considering isopycnal displacements as principal compound event driver.

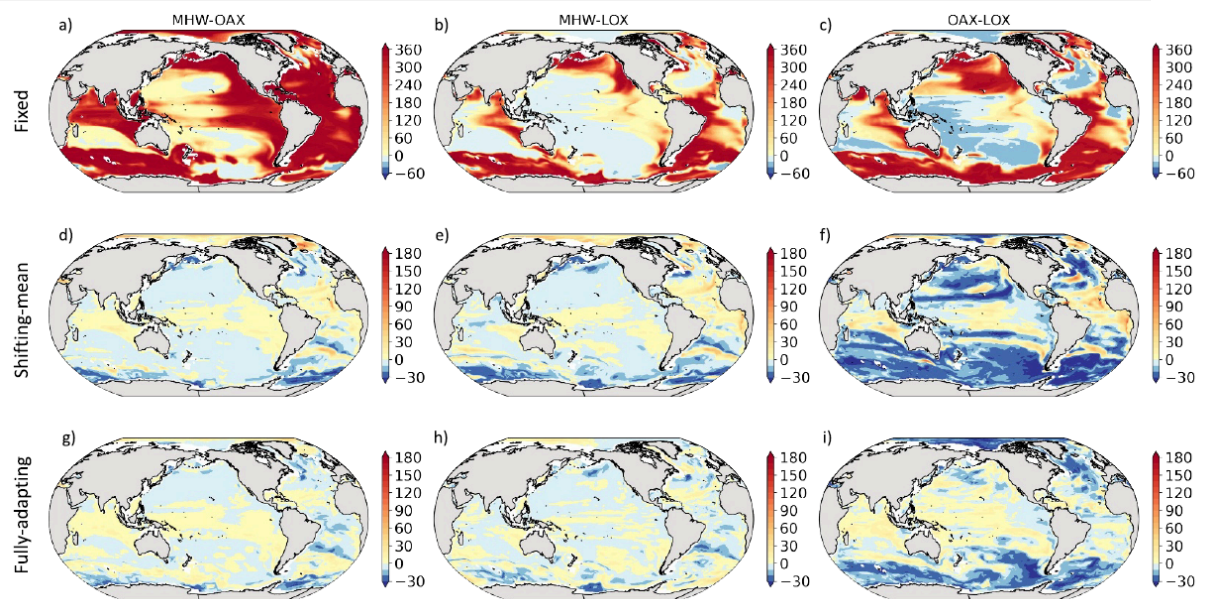


Figure 5 from Legrix et al. 2025. Projected changes in subsurface compound event distribution at 617 m between the preindustrial period and a 2°C warming level in the GFDL-ESM2M large ensemble simulation under RCP8.5. Change in the frequency (days/year) of compound marine heatwave and high acidity (MHW-OAX) events, compound marine heatwave and low oxygen (MHWLOX) events, and compound high acidity and low oxygen (OAX-LOX) events between 1891–1900 and a 11-year period centered around the year when the ensemble mean air surface temperature has reached +2°C, using a (first row) fixed, second row) shifting-mean, and (third row) fully adapting baseline. Note that the color scale differs between panels.



## 5. Part III – Evolution of causal relationships under climate change : controls of Net Primary Productivity in the North Atlantic Subpolar Gyre

### Introduction

Understanding how climate change affects marine primary productivity requires examining the evolving causal relationships between physical and biogeochemical processes. Earth System Models (ESMs) show significant uncertainties in their Net Primary Productivity (NPP) projections (Kwiatkowski et al., 2020 ; Tagliabue et al 2021), particularly in the North Atlantic Subpolar Gyre where inter-model spread exceeds the uncertainty based on emission scenarios (Kwiatkowski et al., 2020).

This region presents particularly interesting characteristics for studying these complex interactions. It hosts highly productive ecosystems characterized by intense spring blooms and pronounced seasonal cycles. Winter vertical mixing constitutes a critical mechanism for replenishing surface waters with nutrients from deeper layers (D'Asaro, 2008; Williams et al., 2006), thus setting the biogeochemical conditions for vigorous spring blooms characteristic of temperate subpolar regions.

Climate change is already modifying this system, with documented freshening and cooling trends (Holliday et al., 2020) that have the potential to alter circulation patterns and, consequently, nutrient distributions (Hatun et al., 2017). The intensification of upper-ocean stratification, projected to increase by 16-30% globally by 2100 (Fu et al., 2016), emerges as an important driver of change, potentially inhibiting nutrient replenishment during productive periods (Behrenfeld et al., 2006; Bopp et al., 2013).

### Method

#### Sliding window approach

This study uses the PCMCI+ causal discovery algorithm (Runge et al., 2019) applied to five Earth System Models (IPSL-CM6A-LR, CESM2, CMCC-ESM2, UKESM1-0-LL and CanESM5-CanOE) (Boucher et al., 2020; Danabasoglu et al., 2020; Lovato et al., 2022; Sellar et al., 2019; Swart et al., 2019) to analyze the evolution of causal relationships between physical and biogeochemical variables. To address the non-stationarity inherent to climate change scenarios, a 100-year sliding window approach is implemented.

This methodology allows to:

- Reduce the impact of non-stationarity within each analysis window
- Investigate the temporal evolution of causal relationships
- Provide a distribution of causal link strengths under different scenarios



The analysis compares historical simulations (1850-2015) with three future scenarios of increasing intensity: SSP126 (low), SSP245 (medium) and SSP585 (high) (Riahi et al., 2017). The last 35 sliding windows are used as reference for the final scenario state, as more than half of the years in these windows belong to the scenario period.

### Conceptual scheme

The conceptual scheme focuses on the eastern part of the subpolar gyre with a specific set of variables. The intensity of NPP during spring bloom serves as the target variable, represented by the maximum productivity reached during bloom.

The analyzed variables include:

- **Atmospheric variables:** North Atlantic Oscillation (NAO) as the primary atmospheric driver
- **Physical variables:** winter Mixed Layer Depth (MLD), spring stratification, gyre strength and horizontal nutrient transport
- **Biogeochemical variables:** four nutrients (nitrate, silicate, dissolved iron and phosphate) calculated as maximum values in the upper water column (100m) reached before bloom initiation

Nutrient transport is calculated across a fixed section at 33°W between 46.5°N and 57.5°N to capture intense circulation patterns along the southern boundary of the subpolar gyre.

## Results

### Evolving role of stratification

While some models maintain unchanged dynamics, others show evolving relationships under climate change scenario.



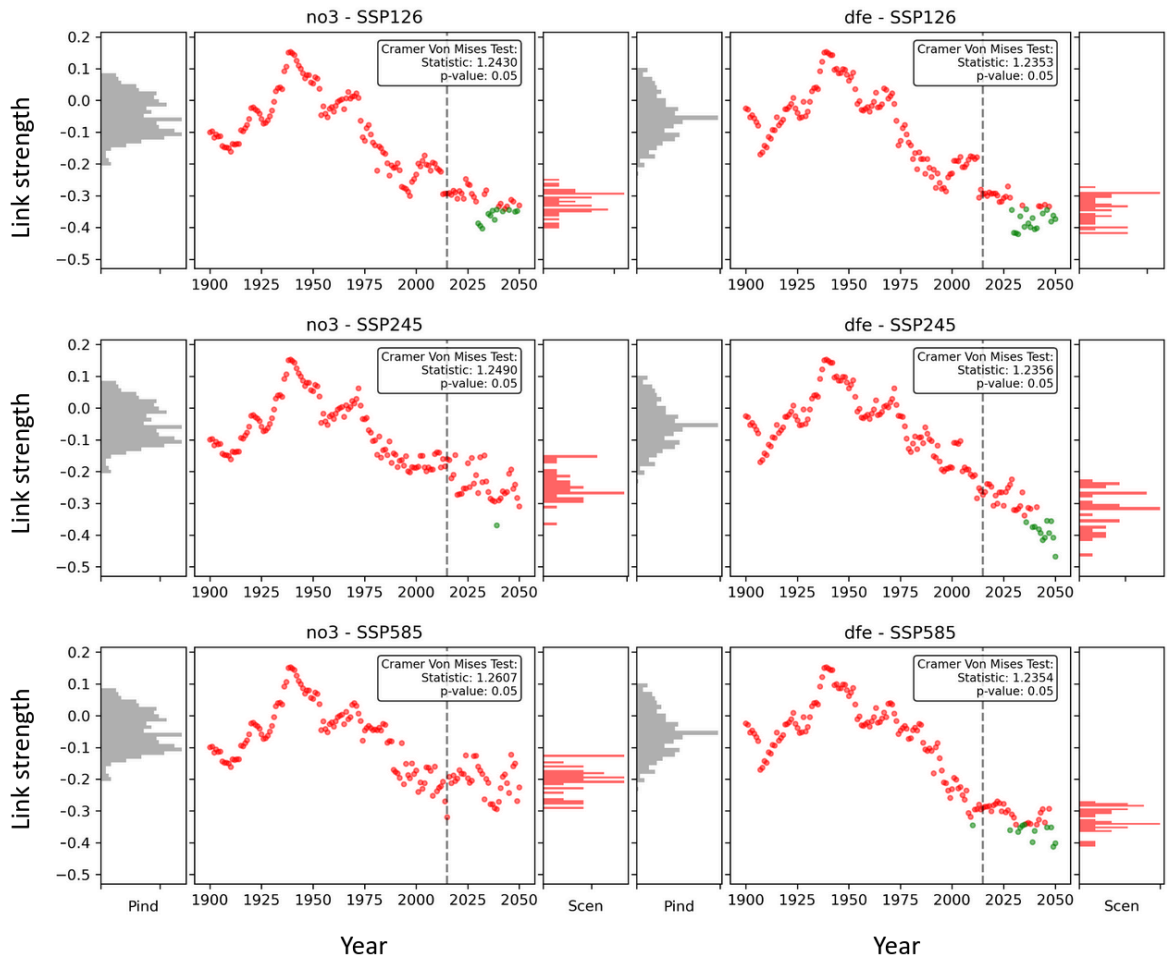


Figure 1: Evolution of the link stratification/net primary productivity for each scenario for CanESM5- CanOE. Each row corresponds to a scenario. The first column corresponds to nitrate and the second one to iron. On the leftmost part of each column, the grey histograms illustrate the strength of the link for a pre-industrial simulation. The scatter plots represent the strength evolution under each scenario, with red indicating non-significant and green indicating significant relationships. Additional red histograms (rightmost part of each column) display the distribution of the relationship strength, based on the last 35 windows of the scenario.

Figure 1 illustrates the evolution of the stratification-NPP link for CanESM5-CanOE across all scenarios. This model exemplifies the emergence of a significant negative relationship between stratification and NPP under climate change scenarios. Across all scenarios, the link strength deviates from the pre-industrial distribution in recent years, reaching a significant strength of approximately -0.4. The trend in relationship strength, calculated from 1940 to the end of the simulation period, ranges between  $-4.5 \times 10^{-3}$  and  $-4.9 \times 10^{-3}$  per year depending on the scenario.

CMCC-ESM2 exhibits a similar pattern across all scenarios, with a significant negative link between stratification and primary productivity outside the pre-industrial distribution, also



reaching approximately -0.4 strength. However, the evolution occurs more rapidly over a shorter period, with trends from 1940 to 1970 ranging from  $-1.25 \times 10^{-2}$  to  $-1.45 \times 10^{-2}$  per year.

Importantly, models with unchanged dynamics still experience climate impacts. For UKESM1-0-LL, while the stratification-NPP link remains stable at approximately -0.7, the stratification increases and the NPP decreases reflecting the strong link between those variables.

This analysis reveals that models are converging toward a consensus under climate change scenarios. Models that initially exhibited weaker stratification-NPP links show increasing intensities over time, thereby narrowing the dispersion between models and suggesting that enhanced stratification impacts represent a robust feature of future ocean productivity changes.

### Nutrient-productivity relationships

The contribution of nutrient variability to NPP projections shows diverse responses across models and nutrients. CanESM5-CanOE demonstrates contrasting evolutions between nutrients: while iron maintains strength values within the pre-industrial distribution, nitrate shows a clear emerging dynamic starting around 1960, with strength increasing to approximately 0.6 under climate scenarios.

IPSL-CM6A-LR exhibits significant strengthening of nutrient-NPP relationships under SSP585, particularly for silicate and phosphate, reaching values outside pre-industrial ranges. Conversely, CMCC-ESM2 shows weakening relationships, with declining link strengths for nitrate, phosphate and silicate over 2020-2050, suggesting a decreasing contribution of nutrients to NPP variability control.

### Compensation mechanisms and transport

A particularly striking finding emerges from IPSL-CM6A-LR, which demonstrates a shift from vertical mixing dominance to enhanced horizontal transport control. While the MLD-nutrient relationship weakens, the transport-nutrient relationship strengthens considerably reaching values close to 0.4 at the end of the scenario. This compensation mechanism helps maintain nutrient availability despite reduced vertical mixing, moderating the expected decline in primary productivity under increased stratification.

These divergent pathways reveal that nutrient dynamics have uncertain evolution across models, with some developing compensation mechanisms while others experience more direct climate constraints, contributing to the large uncertainty in NPP projections for this region.

### Conclusion

This causality-based analysis reveals significant heterogeneity in how Earth System Models represent the evolution of physical-biogeochemical interactions under climate change. While models converge toward a consensus on stratification effects - with initially weaker relationships strengthening over time - they diverge considerably in nutrient supply mechanisms and transport dynamics.



The identification of compensation mechanisms, particularly the shift from vertical mixing to horizontal transport control in IPSL-CM6A-LR, provides new insights into the sources of uncertainty in marine productivity projections. Some models demonstrate resilience through alternative nutrient pathways, while others experience more direct constraints from enhanced stratification.

These findings highlight the importance of understanding model-specific dynamics in causal relationships rather than relying on classical analysis. The causality-based approach identifies mechanisms that traditional analyses miss, offering a novel framework for model intercomparison and understanding ecosystem responses to climate change. This mechanistic understanding is crucial for improving confidence in future projections and identifying which physical processes require better representation in Earth System Models.



## 6. General Conclusion and Perspectives

Deliverable D8.1 provides an integrated assessment of future ecosystem drivers and stressors shaping Atlantic marine ecosystems, with a particular emphasis on regime shifts and tipping-point risk. By combining genomic evidence of biological vulnerability, projections of compound extreme events, and causal analyses of ecosystem regulation, this deliverable identifies where, how, and why Atlantic ecosystems may become less resilient under climate change.

A first key outcome is the demonstration that planktonic communities, central to Atlantic productivity and biogeochemical functioning, are likely to undergo major spatial and functional reorganization as environmental conditions depart from present-day envelopes. Genomic province projections indicate substantial redistribution driven primarily by warming, with contributions from nutrients and salinity, implying widespread shifts in community structure and, consequently, in ecosystem functioning. Complementarily, metatranscriptomic analyses across the Atlantic–Arctic transition show that sharp environmental gradients (notably at the polar front) are associated with strong functional differentiation and convergent stress-response signatures across distinct phytoplankton lineages, highlighting both the capacity for acclimation and the likelihood of selective filtering under intensified “Atlantification”. Together, these results position genomic and transcriptomic signals as early-warning indicators of ecosystem destabilization.

A second major result is the quantification of the growing threat posed by compound marine extremes, which act as powerful stress multipliers beyond single-variable anomalies. The co-occurrence of marine heatwaves with high acidity, and, in subsurface layers, with hypoxia, emerges as a critical class of events capable of inducing non-linear ecosystem responses. Projections indicate strong increases in the frequency and spatial footprint of these compound extremes under warming, including at depth, reinforcing the idea that tipping risks are three-dimensional and not restricted to surface habitats. This reinforces the need to frame future ecosystem vulnerability in terms of compound exposure rather than isolated drivers.

Third, the causal discovery analysis of the North Atlantic subpolar gyre shows that climate change is likely to reshape the causal architecture that governs net primary productivity. Across models, stratification tends to exert an increasingly negative control on productivity, while nutrient–productivity links and transport pathways display model-dependent trajectories, including evidence for compensation mechanisms (e.g., strengthened horizontal transport partially offsetting weakened vertical mixing in some configurations). This causal perspective is essential for tipping-point assessment because it does not only track trends in state variables, but detects changes in controlling mechanisms, a hallmark of approaching thresholds and regime shifts.



## Perspectives.

D8.1 highlights the value of integrating (i) molecular-scale indicators of vulnerability, (ii) compound-extreme diagnostics, and (iii) causal-mechanistic analyses to build a coherent risk framework for regime shifts in Atlantic ecosystems. Future work should prioritize: (1) translating these results into regional vulnerability maps and monitoring priorities (including subsurface risk); (2) strengthening model evaluation and intercomparison around process-level controls (mixing, stratification, transport, nutrient limitation); and (3) developing early-warning indicators that combine genomic signals, compound-stressor exposure, and changes in causal link structure. Overall, D8.1 provides the scientific basis to anticipate ecosystem instability under climate forcing and to better target observation–model integration for robust risk assessment.



## 7. References

Behrenfeld, M. J., O'Malley, R. T., Siegel, D. A., McClain, C. R., Sarmiento, J. L., Feldman, G. C., Milligan, A. J., Falkowski, P. G., Letelier, R. M., & Boss, E. S. (2006). Climate-driven trends in contemporary ocean productivity. *Nature*, 444(7120), 752–755.

Bopp, L., Resplandy, L., Orr, J. C., Doney, S. C., Dunne, J. P., Gehlen, M., Halloran, P., Heinze, C., Ilyina, T., Séférian, R., et al. (2013). Multiple stressors of ocean ecosystems in the 21st century: projections with CMIP5 models. *Biogeosciences*, 10(10), 6225–6245.

Boucher, O., Servonnat, J., Albright, A. L., Aumont, O., Balkanski, Y., Bastrikov, V., et al. (2020). Presentation and evaluation of the IPSL-CM6A-LR climate model. *Journal of Advances in Modeling Earth Systems*, 12(7), e2019MS002010.

Burger, F.A., Terhaar, J. & Frölicher, T.L. Compound marine heatwaves and ocean acidity extremes. *Nat Commun* 13, 4722 (2022).

Danabasoglu, G., Lamarque, J.-F., Bacmeister, J., Bailey, D. A., DuVivier, A. K., Edwards, J., et al. (2020). The Community Earth System Model Version 2 (CESM2). *Journal of Advances in Modeling Earth Systems*, 12(2), e2019MS001916.

D'Asaro, E. A. (2008). Convection and the seeding of the North Atlantic bloom. *Journal of Marine Systems*, 69(3-4), 233–237.

Frémont, P., Gehlen, M., Vrac, M., Leconte J., Delmont T., Wincker P., Iudicone D., Jaillon O, Restructuring of plankton genomic biogeography in the surface ocean under climate change. *Nat. Clim. Chang.* 12, 393–401 (2022).

Frémont P., Pelletier E., Da Silva C., Oziel L., Campese L., Villar E., Vannier T., Rastogi A., Aury JM., Karp Boss L., Babin M., Wincker P, BowlerC., Gehlen M., Iudicone D., Jaillon O., Changes in gene expression in eukaryotic phytoplankton at the Atlantic-Arctic polar front. bioRxiv (2025).

Fu, W., Randerson, J. T., & Moore, J. K. (2016). Climate change impacts on net primary production (NPP) and export production (EP) regulated by increasing stratification and phytoplankton community structure in the CMIP5 models. *Biogeosciences*, 13(18), 5151–5170.

Hjalmar Hatun, K Azetsu-Scott, R Somavilla, Francisco Rey, C Johnson, Moritz Mathis, Uwe Mikolajewicz, P Coupel, J-E Tremblay, S Hartman, et al. The subpolar gyre regulates silicate concentrations in the north atlantic. *Scientific reports*, 7(1):14576, 2017.

Holliday, N. P., Bersch, M., Berx, B., Chafik, L., Cunningham, S., Florindo-López, C., et al. (2020). Ocean circulation causes the largest freshening event for 120 years in eastern subpolar North Atlantic. *Nature Communications*, 11(1), 585.



Kwiatkowski, L., Torres, O., Bopp, L., Aumont, O., Chamberlain, M., Christian, J. R., et al. (2020). Twenty-first century ocean warming, acidification, deoxygenation, and upper-ocean nutrient and primary production decline from CMIP6 model projections. *Biogeosciences*, 17(13), 3439–3470.

Le Grix, N., Burger, F. A., & Frölicher, T. L. (2025). Surface and subsurface compound marine heatwave and biogeochemical extremes under Climate change. *Global Biogeochemical Cycles*, 39, e2025GB008514.

Lovato, T., Peano, D., Butenschön, M., Materia, S., Iovino, D., Scoccimarro, E., et al. (2022). CMIP6 simulations with the CMCC Earth System Model (CMCC-ESM2). *Journal of Advances in Modeling Earth Systems*, 14(3), e2021MS002814.

Riahi, K., van Vuuren, D. P., Kriegler, E., Edmonds, J., O'Neill, B. C., Fujimori, S., et al. (2017). The Shared Socioeconomic Pathways and their energy, land use, and greenhouse gas emissions implications: An overview. *Global Environmental Change*, 42, 153–168.

Runge, J., Nowack, P., Kretschmer, M., Flaxman, S., & Sejdinovic, D. (2019). Detecting and quantifying causal associations in large nonlinear time series datasets. *Science Advances*, 5(11), eaau4996.

Sellar, A. A., Jones, C. G., Mulcahy, J. P., Tang, Y., Yool, A., Wiltshire, A., et al. (2019). UKESM1: Description and evaluation of the UK Earth System Model. *Journal of Advances in Modeling Earth Systems*, 11(12), 4513–4558.

Swart, N. C., Cole, J. N. S., Kharin, V. V., Lazare, M., Scinocca, J. F., Gillett, N. P., et al. (2019). The Canadian Earth System Model version 5 (CanESM5.0.3). *Geoscientific Model Development*, 12(11), 4823–4873.

Williams, R. G., Roussenov, V., & Follows, M. J. (2006). Nutrient streams and their induction into the mixed layer. *Global Biogeochemical Cycles*, 20(1).

